Hindawi Publishing Corporation
Journal of Nanomaterials
Volume 2016, Article ID 5697672, 7 pages
http://dx.doi.org/10.1155/2016/5697672

Research Article

Facile Synthesis of High {001} Facets Dominated BiOCl Nanosheets and Their Selective Dye-Sensitized Photocatalytic Activity Induced by Visible Light

Da Zhang,[1,2] Liang Chen,[1,2] Chengjing Xiao,[1,2] Jing Feng,[1,2] Lingmin Liao,[1,2] Zaiqin Wang,[1,2] and Tao Wei[1,2]

[1]*Materials and Structural Department, Changjiang River Scientific Research Institute, Wuhan 430010, China*
[2]*Collaborative Innovation Center for Geo-Hazards and Eco-Environment in Three Gorges Area, Yichang 443002, China*

Correspondence should be addressed to Da Zhang; zhangda@mail.crsri.cn and Zaiqin Wang; wangzq@mail.crsri.cn

Received 4 October 2015; Revised 16 December 2015; Accepted 20 December 2015

Academic Editor: Takuya Tsuzuki

Single-crystal BiOCl nanosheets, with high {001} facets exposed, were synthesized through a facile hydrolysis reaction under general atmospheric pressure, without adding any organic surfactant or agent. The thickness of the BiOCl nanosheets is about 20 nm, and the diameter is arranged from 200 to 400 nm. The structure of the BiOCl nanosheets was characterized by X-ray diffraction, energy disperse X-ray spectrum, transmission electron microscopy, and selective area electron diffraction. Moreover, three different dyes were used as model molecules to test the photocatalytic activity of BiOCl nanosheets under visible light. It was found that the BiOCl nanosheets possess selective photocatalytic behavior as their activity over RhB is much higher than that over MO or MB. Based on the analysis of the experimental results, the potential mechanism was discussed.

1. Introduction

With the development of modern industrial society, environmental pollution and energy shortage have evolved into a global crisis. As a green method, photocatalytic technology has the advantages of low cost and high efficiency and does not produce secondary pollution, which has broad potential application prospect in solving the environmental problems [1]. The structural design and catalytic mechanism of semiconductor photocatalytic materials have attracted much interest of chemistry and materials researchers [2, 3]. Most semiconductor photocatalytic materials can only be induced by UV light, which accounts for only a small part of the sunlight. The exploration of catalysts with high activity under visible light is a hot research area [4–6].

However, some ultraviolet light photocatalysts could degrade dye solution under visible light because of dye-sensitized photocatalytic process [7–9]. Liu et al. did much research about the catalytic mechanism of TiO_2 in degrading different dye solution. After the particle surface of TiO_2 nanoparticles was treated by fluorine, the dye adsorption and degradation effects have obvious difference [10]. They also used many kinds of measurements to detect the intermediate active substances and degradation products [11, 12]. In addition, the relevant research about photosensitized catalytic activity of other UV light photocatalytic materials under visible light is not common.

Bismuth oxide chloride (BiOCl) is a highly anisotropic layered structure of semiconductor [13–16]. The crystal structure is derived from a tetragonal matlockite structure, in which one bismuth atom coordinates with four oxygen atoms in one base and four chlorine atoms in another. One oxygen atom coordinates with four bismuth atoms and so does the chlorine atom, thus forming the BiOCl crystal [17, 18]. The tetragonal $[Bi_2O_2]$ structure is combined by two chlorine slabs to get a "sandwich" layer and different layers are stacked together by the nonbonding interaction (van der Waals). It is the indirect transition band gap semiconductor, with the band gap of about 3.27 eV. In most literatures, the photocatalytic activity was tested under ultraviolet light because of its large band gap width.

In this work, a facile hydrolysis method, without any capping agent added, is explored to synthesize BiOCl single-crystal nanosheets. The most highly exposed facet was detected to be {001} facets. Three different dyes were used to discuss the photocatalytic activity under visible light. It was found that degradation efficiency of RhB is much higher than MO or MB under visible light. Because the BiOCl material belongs to large band gap photocatalysts, it cannot be excited by visible light. The mechanism of BiOCl nanosheets degrading the dyes solution was concluded by visible light sensitized photocatalytic process. More interestingly, the degradation efficiency of these BiOCl nanosheets over RhB is much higher than that over MB or MO, showing high selective photocatalytic activity. It should be emphasized that till now there are some researches on the selective photocatalysts under UV light [19–21] and rare report on the selective photocatalysts under visible light [22, 23]. The investigation of selective activities of semiconductors is important for better understanding of the mechanism of photocatalytic process, which also better direct the exploring of more efficient visible light induced photocatalysts.

2. Experimental Section

2.1. Materials. $Bi(NO_3)_3{\cdot}5H_2O$, NaCl, ethanol, RhB, MO, and MB were of analytical grade and purchased from Shanghai Chemical Reagent Ltd. 5,5-Dimethyl-1-pyrroline-N-oxide (DMPO) was purchased from Sigma-Aldrich Chemical Company.

2.2. Synthesis of BiOCl Nanosheets. All samples were prepared via a hydrolysis process. As for the synthesis of BiOCl nanosheets, 0.0585 g (1 mmol) of NaCl was dissolved in 15 mL deionized water in a three-neck flask and heated to 90°C. Then 0.4858 g (1 mmol) of $Bi(NO_3)_3{\cdot}5H_2O$ was dispersed into 20 mL ethanol by ultrasonation to get a suspension which was then added to the above NaCl solution under 90°C dropwise. The reaction was maintained at the same temperature for 3 h and then cooled to room temperature naturally. The precipitation was separated by centrifugation and washed with deionized water and absolute ethanol several times, respectively. Finally, the as-obtained product was dried under vacuum at 60°C for further characterization.

2.3. Characterization. XRD patterns of samples were measured on a Bruker D8-advance X-ray diffractometer with Cu Kα radiation (λ = 0.154056 nm) (Germany), using a voltage of 40 kV, a current of 40 mA, and a scanning rate of 0.02°/s, in 2θ ranges from 10° to 70°. The cell lattice constants of samples were calculated and corrected by MDI Jade (5.0 edition) software. SEM images were acquired on a Hitachi S-4800 scanning electron microscope (SEM). Transmission electron microscopy (TEM, JEM-2100, JEOL) with fast Fourier transformation (FFT) and selected area electron diffraction (SAED) was measured at an accelerating voltage of 200 KV. UV-visible diffuse reflectance absorbance (DRS) and Raman spectra were obtained with UV-vis diffuse reflectance spectrometer (BWS003, Newark, DE) and a Raman spectrometer (inVia, Renishaw), respectively. The EPR results were obtained on electron paramagnetic resonance spectrometer (EPR, ER200-SRC-10/12, Bruker), with an in situ irradiation system.

2.4. Photocatalytic Degradation Measurement. The photocatalytic degradation experiments of the obtained BiOCl products for the decomposition of 20 mg/L RhB (or 10 mg/L MB, 10 mg/L MO) in aqueous solution were performed in XPA-Photochemical Reactor (Xujiang Electromechanical Plant, Nanjing, China). A 500 W Xenon lamp with a filter ($\lambda \geq 400$ nm) was used to obtain visible light, and the near-infrared light was removed by condensate water around the lamp. A mixture of 40 mL of 20 mg/L RhB aqueous solution and 40 mg of BiOCl powder was transferred into a quartz tube with a capacity of 50 mL. The above suspension was treated by ultrasonation for 10 min and then magnetically stirred in dark for 1 h to reach adsorption equilibrium of RhB with the catalyst. Then the mixture was continuously agitated throughout the experiment and irradiated by the visible light. After a given irradiation time, about 3 mL of the mixture was withdrawn and immediately centrifuged to remove the catalyst. The concentration of dye solution was determined by measuring its absorption in the main absorbance with UV-vis spectrophotometer (Agilent 8453).

3. Results and Discussion

The general morphology of the as-prepared BiOCl nanosheets was characterized by SEM and TEM as shown in Figure 1, which is irregular nanosheet structure. The size of the nanosheets is about 200–400 nm, and the thickness is about 20 nm. Further analyses of BiOCl nanosheets have been characterized by high resolution transmission electron microscope (HRTEM) and selected area electron diffraction (SAED). The HRTEM image for a single nanosheet is showed in Figure 1(d) and we got corresponding SAED spot patterns at the according part of the nanosheet, showing that each nanosheet is single-crystal and owns high crystallinity. The main exposed surface of the BiOCl nanosheets could be confirmed to be {001} facets based on the analysis of SAED results. The interplaner spacing of 0.275 nm well corresponds with the (110) plane of tetragonal BiOCl crystal.

The phase and composition of the BiOCl nanosheets, which was prepared by the hydrolysis reaction, were investigated by XRD pattern (Figure 2). The intense and clear diffraction peaks imply the good crystallinity of the as-prepared BiOCl sample. All diffraction peaks can be indexed to pure tetragonal phase (JCPDS 06-0249, space group: P4/nmm, unit cell parameters: a = 3.893 Å, b = 3.893 Å, and c = 7.363 Å). There is no other diffraction peaks, showing that the purity of BiOCl sample prepared by this method is high. A great increase in the relative intensity of (001), (002), (003), (004), and (006) peaks can be found in the spectrum. The peak (001) in BiOCl sample is obviously the strongest one, contrary to 40% intensity in the standard spectrum. The relative intensities of all (001) series facets are higher than those in the standard spectrum, indicating the highly exposed (001) facets of BiOCl nanosheets, which is in good accordance with the HRTEM and SEAD results in the previous discussion [18].

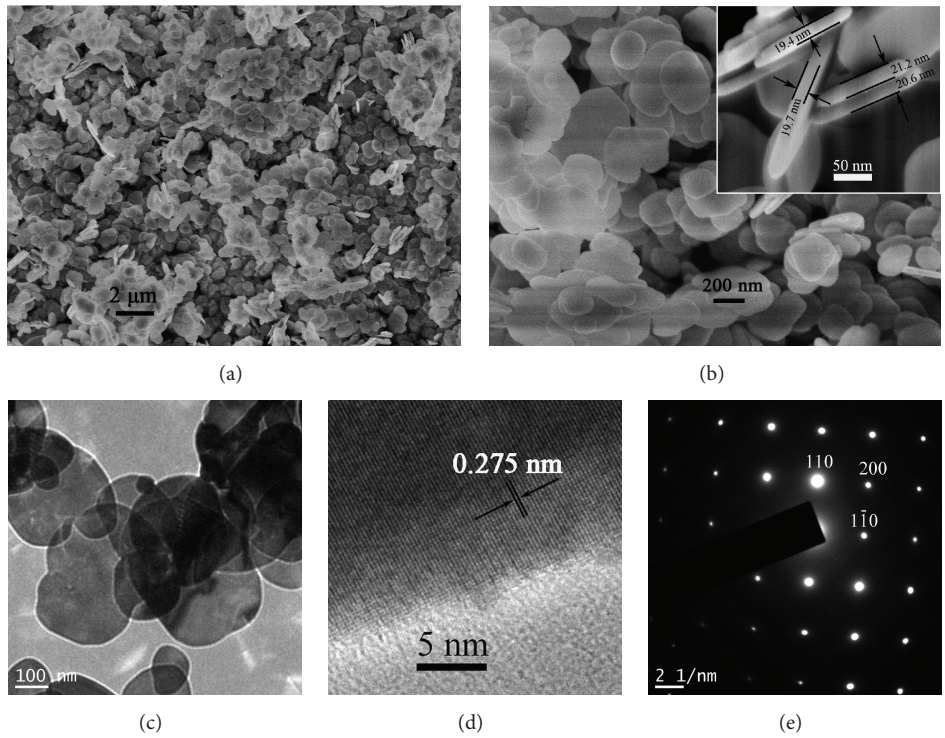

Figure 1: Morphologies of the BiOCl nanosheets. (a, b) SEM images, (c) TEM image, (d) HRTEM image, and (e) corresponding SEAD pattern.

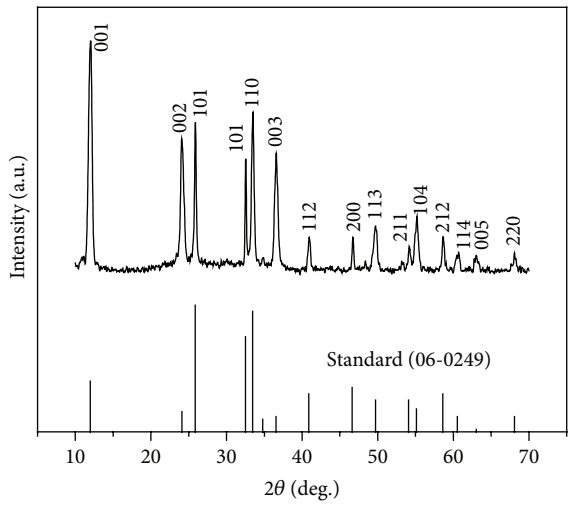

Figure 2: XRD patterns of the BiOCl nanosheets.

The UV-vis diffuse reflectance spectrum (DRS) of the as-prepared BiOCl nanosheets is shown in Figure 3. It has one absorption peak located around 320 nm, which could be contributed to the excitation band edge emission. It is reported that BiOCl exhibits an indirect band gap. In Figure 3(b), plots of $(Ah\nu)^{1/2}$ versus the energy of absorbed light ($h\nu$) afford the band gaps of as-prepared BiOCl nanosheets, where A is the absorbance and $h\nu$ is the discrete photon energy [13]. The extrapolated value of $h\nu$ at $A = 0$ gives an absorption edge energy corresponding to the band gap. The band gap width of BiOCl sample is about 3.22 eV belonging to ultraviolet light region, and this is also consistent with the appearance of the BiOCl sample which looks white.

The photocatalytic efficiency of BiOCl nanosheets under visible light was studied using three kinds of dye (RhB, MO, and MB, in Figure 4) as model molecules. From the changes of dye concentrations in Figure 5, the BiOCl nanosheets show good adsorption performance and photocatalytic effect with RhB solution. About 43% of RhB molecules were adsorbed under dark condition. With visible light treatment, the concentration of RhB solution declined rapidly. 94% of dye molecules were removed after 30 min, and the solution becomes transparent in 45 min. As for MB solution, the BiOCl nanosheets show good adsorption property but bad photocatalytic activity. The solution concentration under adsorption equilibrium reduced to only 27% of the initial value. After 2 h of visible light treatment, the MB dye concentration was basically unchanged. For the MO solution, the BiOCl nanosheets show bad adsorption performance and limited catalytic effect. The dye concentration is 92% of the initial value under adsorption equilibrium. With visible light irradiation, the MO concentration declined slowly, and, after 2 h of irradiation, the concentration reduced to 79% of the initial value. We excluded the adsorption amount to calculate the real photocatalytic activity in Figure 5(d), and it could be found that the BiOCl nanosheets possess selective photocatalytic behavior as their activity over RhB is much higher than that over MO or MB.

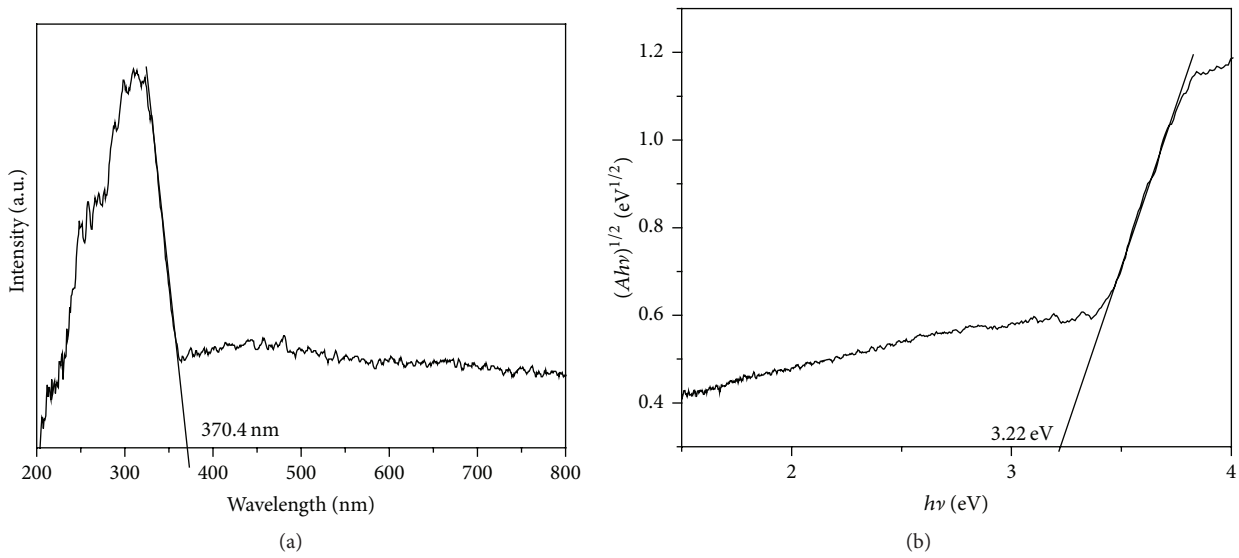

Figure 3: (a) UV-visible diffuse reflectance spectra of the BiOCl nanosheets and (b) the according band gap calculated by the DRS results.

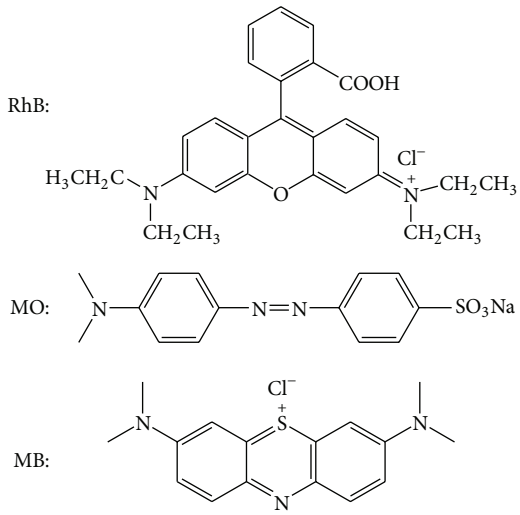

Figure 4: The molecular structures of three different dyes.

Based on the adsorption and catalytic processes of three different dyes, we could find that the BiOCl nanosheets performed good adsorption effect over RhB and MB molecules, and the reason is related to the crystal structure and surface properties of BiOCl nanosheets. The BiOCl crystal easily dissociated along [001] direction and so exposed the Cl atomic layer with negative charge, which has stronger acting force to RhB and MB molecules with the positive charge in solution and has weak acting force to MO molecule with negative charge. When irradiated by visible light, the concentration of RhB solution decreased sharply with BiOCl nanosheets, achieving rapid degradation efficiency, while, for the MB molecular, the concentration was basically unchanged, and it cannot be degraded by BiOCl nanosheets under visible light. For MO molecule, BiOCl nanosheets have certain photocatalytic effect, which is far weaker than that over RhB solution.

The BiOCl nanosheets cannot be excited by visible light due to its wide band gap based on the DRS analysis. There are no photogenerated electrons and holes under visible light, which is also confirmed by ESR results in Figure 6. The electron trapping agent DMPO was used for detection of active radicals in the BiOCl dispersion under visible light or ultraviolet light. The results showed that BiOCl nanosheets only were excited by ultraviolet light and cannot produce hydroxyl radical under visible light irradiation. However, the BiOCl nanosheets have some catalytic effect over RhB and MO. The photocatalytic mechanism could be attributed to dye-sensitized degradation process.

The dye molecules as photosensitized substances can stimulate the photocatalytic activity of catalysts. The dye-sensitized photocatalytic process was usually described as follows (Figure 7). Firstly, dye molecules absorbed photons and formed excited singlet or triplet state under visible light irradiation. Following the dye molecules in excited state injected electron into the conduction band of semiconductor, and simultaneously they became a positive carbon radicals. Then the injected electrons were captured by O_2 on the surface of semiconductor. So the superoxide radicals and other reactive oxygen radicals formed. These active species attacked carbon radicals, generated hydroxylated products, and finally broke down the organic molecules into CO_2, H_2O, and other small molecules. The electronic excitation is obtained through the transmission between the adsorbed dye molecules and the conduction band of semiconductor. The mechanism of dye-sensitized photodegradation has been recovered in the presence of TiO_2 by Wu et al. [8], but the selective photocatalytic property of other photocatalysts besides TiO_2 is rarely discussed in literatures. We also used TiO_2 as photocatalysts under the same visible light but dye-sensitized photocatalytic process did not happen.

In the presence of BiOCl nanosheets, three kinds of dye molecules' removal rates have the following sequence of RhB > MO > MB. There are two main reasons. One is the charge

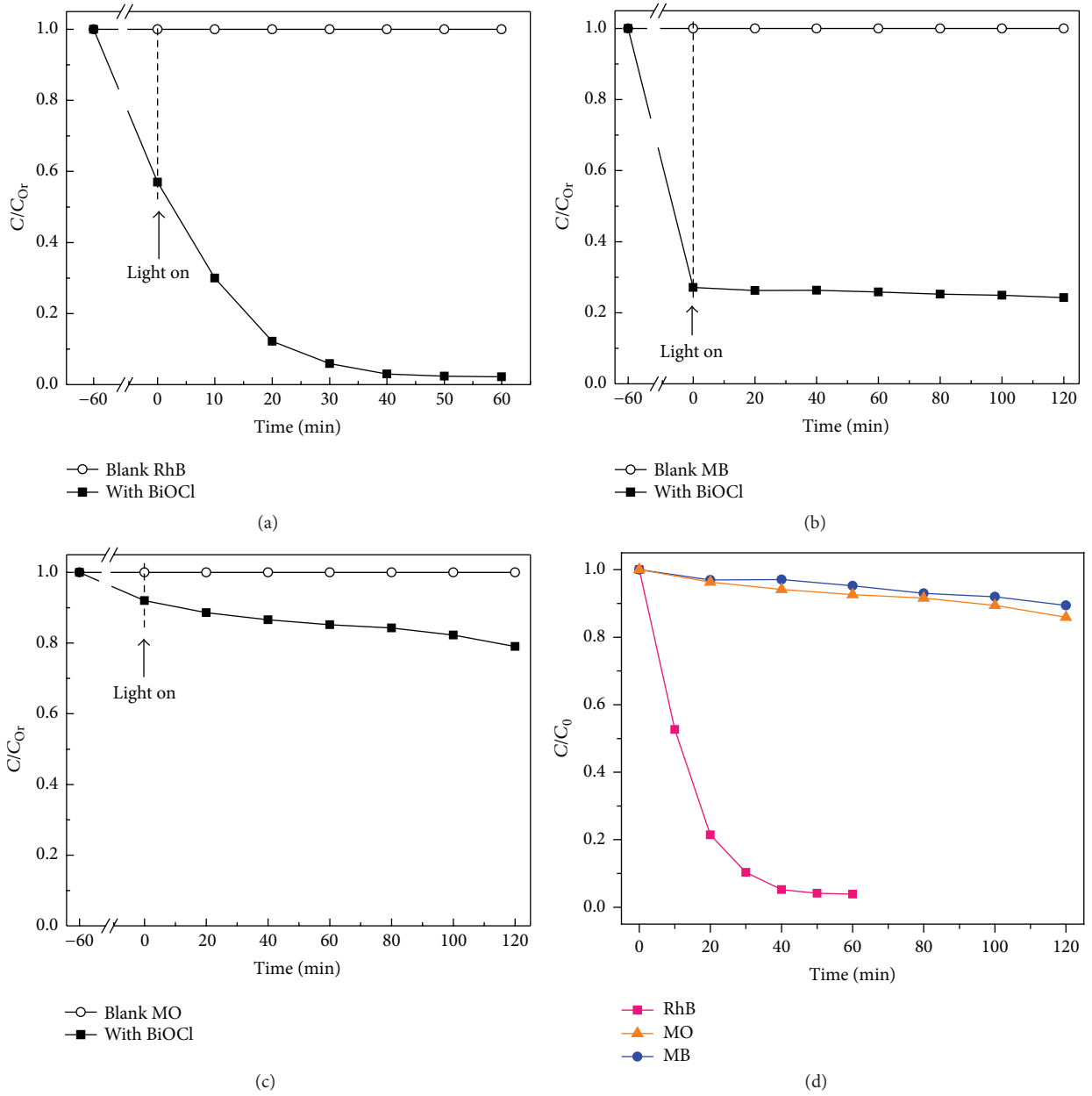

FIGURE 5: (a) The concentration changes (C/C_{Or}, detected concentration/original concentration) of RhB in the presence of BiOCl nanosheets under visible light. The concentration changes of MB (b) and MO (c). The photocatalytic activity of BiOCl nanosheets over the three dyes (d).

of the dye molecules. Photocatalytic reaction occurs at the surface of the semiconductor materials. The Zeta potential result of BiOCl nanosheets dispersed in water (Figure 8) shows that the BiOCl nanosheets are negatively charged (−12.6 mV) on their surfaces. Since the RhB is positively charged and it is easy to be absorbed by BiOCl nanosheets because of electronic effect the electrons produced by dye photosensitized transfer more easily between dye molecules and photocatalysts, showing high catalytic efficiency. While MO is not easy to be adsorbed, the occurrence rate of charge transfer is smaller. The other reason is due to the structural stability of dye molecules. Based on the molecular structure analysis of three dyes, MB is the most stable molecule, in which three rings are conjugated, and there are few reports on the degradation of MB under visible light at present. The conjugated structure of MO molecule formed by n-n bonds is in the middle, and the conjugated degree of RhB molecule is the weakest. That is why the BiOCl nanosheets preformed selective photodegradation ability over the three different dye molecules.

4. Conclusion

In summary, high {001} facets exposed BiOCl nanosheets have been synthesized by a facile hydrolysis reaction under

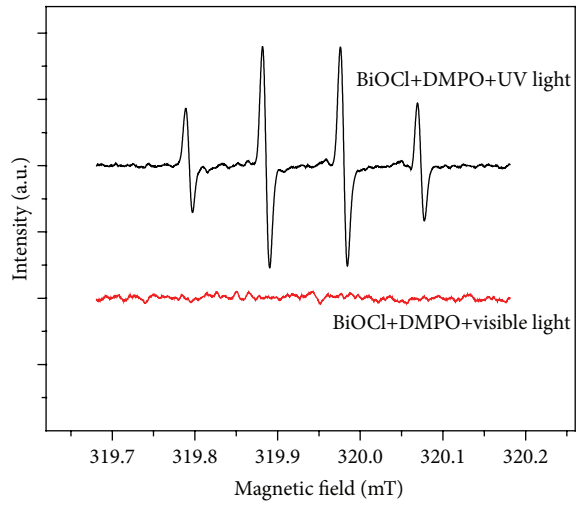

Figure 6: The EPR results of the BiOCl catalysts under visible light and UV light in the presence of DMPO.

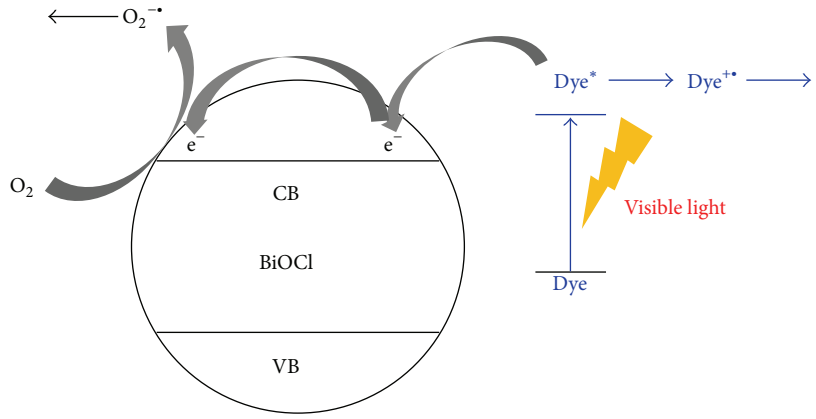

Figure 7: The degradation process of dye molecules under visible light.

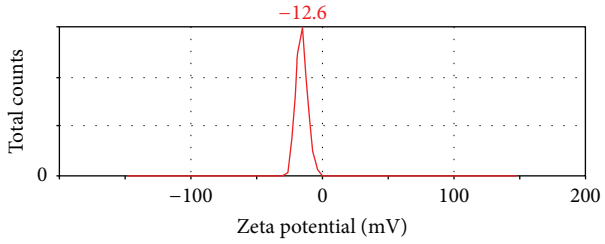

Figure 8: The Zeta potential result of BiOCl nanosheets dispersed in water. It shows that the BiOCl nanosheets are negatively charged (−12.6 mV) on their surfaces.

mild condition. Each BiOCl nanosheet was single-crystal with tetragonal phase. The main exposed surface was confirmed to be {001} facets by TEM and SEAD results. The BiOCl sample shows white color and has no absorption in visible light region. However, the BiOCl photocatalysts possess good degradation effect over RhB solution under visible light. The other two dyes MO and MB were also used as models to investigate the photocatalytic efficiency. Interestingly, the BiOCl product shows high selective photocatalytic activity, as its degradation efficiency over RhB is much higher than that over MB or MO. Furthermore, the mechanism was analyzed and attributed to the charge and the structure stability of dye molecules. This work not only finds a facile method to obtain single-crystal photocatalysts with high active facets exposed but also brings a bright prospect for the mechanism of dye-sensitized photocatalytic process under visible light.

Conflict of Interests

The authors declare that there is no conflict of interests regarding the publication of this paper.

Acknowledgments

This work was supported by National Natural Science Foundation of China (Grant nos. 51209023, 51309018, and 51378078) and Ministry of Water Resources Nonprofit Industry Research Project (Grant no. 201301023). Thanks are due to the supporting by Innovation Team (CKSF2012051/CL)

and the fundamental research funds (CKSF2016020/CL) of Changjiang River Scientific Research Institute.

References

[1] A. Kudo and Y. Miseki, "Heterogeneous photocatalyst materials for water splitting," *Chemical Society Reviews*, vol. 38, no. 1, pp. 253–278, 2009.

[2] Y. Bi, S. Ouyang, N. Umezawa, J. Cao, and J. Ye, "Facet effect of single-crystalline Ag_3PO_4 sub-microcrystals on photocatalytic properties," *Journal of the American Chemical Society*, vol. 133, no. 17, pp. 6490–6492, 2011.

[3] G. Liu, H. G. Yang, X. Wang et al., "Visible light responsive nitrogen doped anatase TiO_2 sheets with dominant 001 facets derived from TiN," *Journal of the American Chemical Society*, vol. 131, no. 36, pp. 12868–12869, 2009.

[4] P. Wang, B. Huang, X. Qin et al., "Ag@AgCl: a highly efficient and stable photocatalyst active under visible light," *Angewandte Chemie—International Edition*, vol. 47, no. 41, pp. 7931–7933, 2008.

[5] D. Zhang, J. Li, Y. Chen, Q.-S. Wu, and Y.-P. Ding, "One-pot preparation and enhanced photocatalytic and electrocatalytic activities of ultralarge Ag/ZnO hollow coupled structures," *CrystEngComm*, vol. 14, no. 20, pp. 6738–6743, 2012.

[6] W. Zhai, S. Xue, A. Zhu, Y. Luo, and Y. Tian, "Plasmon-driven selective oxidation of aromatic alcohols to aldehydes in water with recyclable Pt/TiO_2 nanocomposites," *ChemCatChem*, vol. 3, no. 1, pp. 127–130, 2011.

[7] C. Chen, W. Ma, and J. Zhao, "Semiconductor-mediated photodegradation of pollutants under visible-light irradiation," *Chemical Society Reviews*, vol. 39, no. 11, pp. 4206–4219, 2010.

[8] T. Wu, G. Liu, J. Zhao, H. Hidaka, and N. Serpone, "Evidence for H_2O_2 generation during the TiO_2-assisted photodegradation of dyes in aqueous dispersions under visible light illumination," *Journal of Physical Chemistry B*, vol. 103, no. 23, pp. 4862–4867, 1999.

[9] G. Li, B. Jiang, S. Xiao et al., "An efficient dye-sensitized BiOCl photocatalyst for air and water purification under visible light irradiation," *Environmental Sciences: Processes & Impacts*, vol. 16, no. 8, pp. 1975–1980, 2014.

[10] G. Liu, X. Li, J. Zhao, S. Horikoshi, and H. Hidaka, "Photooxidation mechanism of dye alizarin red in TiO_2 dispersions under visible illumination: an experimental and theoretical examination," *Journal of Molecular Catalysis A: Chemical*, vol. 153, no. 1-2, pp. 221–229, 2000.

[11] G. Liu and J. Zhao, "Photocatalytic degradation of dye sulforhodamine B: a comparative study of photocatalysis with photosensitization," *New Journal of Chemistry*, vol. 24, no. 6, pp. 411–417, 2000.

[12] G. Liu, J. Zhao, and H. Hidaka, "ESR spin-trapping detection of radical intermediates in the TiO_2-assisted photo-oxidation of sulforhodamine B under visible irradiation," *Journal of Photochemistry and Photobiology A: Chemistry*, vol. 133, no. 1-2, pp. 83–88, 2000.

[13] X. Zhang, Z. Ai, F. Jia, and L. Zhang, "Generalized one-pot synthesis, characterization, and photocatalytic activity of hierarchical BiOX (X = Cl, Br, I) nanoplate microspheres," *The Journal of Physical Chemistry C*, vol. 112, no. 3, pp. 747–753, 2008.

[14] H. An, Y. Du, T. Wang, C. Wang, W. Hao, and J. Zhang, "Photocatalytic properties of BiOX (X = Cl, Br, and I)," *Rare Metals*, vol. 27, no. 3, pp. 243–250, 2008.

[15] L. Ye, L. Zan, L. Tian, T. Peng, and J. Zhang, "The 001 facets-dependent high photoactivity of BiOCl nanosheets," *Chemical Communications*, vol. 47, no. 24, pp. 6951–6953, 2011.

[16] H. Cheng, B. Huang, and Y. Dai, "Engineering BiOX (X = Cl, Br, I) nanostructures for highly efficient photocatalytic applications," *Nanoscale*, vol. 6, no. 4, pp. 2009–2026, 2014.

[17] J. Jiang, K. Zhao, X. Xiao, and L. Zhang, "Synthesis and facet-dependent photoreactivity of BiOCl single-crystalline nanosheets," *Journal of the American Chemical Society*, vol. 134, no. 10, pp. 4473–4476, 2012.

[18] D. Zhang, J. Li, Q. Wang, and Q. Wu, "High {001} facets dominated BiOBr lamellas: facile hydrolysis preparation and selective visible-light photocatalytic activity," *Journal of Materials Chemistry A*, vol. 30, no. 1, pp. 8622–8629, 2013.

[19] Y. Shiraishi, N. Saito, and T. Hirai, "Adsorption-driven photocatalytic activity of mesoporous titanium dioxide," *Journal of the American Chemical Society*, vol. 127, no. 37, pp. 12820–12822, 2005.

[20] S. Zhan, D. Chen, X. Jiao, and Y. Song, "Mesoporous TiO_2/SiO_2 composite nanofibers with selective photocatalytic properties," *Chemical Communications*, no. 20, pp. 2043–2045, 2007.

[21] S. Jin, Y. Li, H. Xie, X. Chen, T. Tian, and X. Zhao, "Highly selective photocatalytic and sensing properties of 2D-ordered dome films of nano titania and nano Ag^{2+} doped titania," *Journal of Materials Chemistry*, vol. 22, no. 4, pp. 1469–1476, 2012.

[22] J. Shen, Y. Zhu, X. Yang, and C. Li, "Magnetic composite microspheres with exposed {001} faceted TiO_2 shells: a highly active and selective visible-light photocatalyst," *Journal of Materials Chemistry*, vol. 22, no. 26, pp. 13341–13347, 2012.

[23] Q. Wang, C. Chen, D. Zhao, M. Wanhong, and J. Zhao, "Change of adsorption modes of dyes on fluorinated TiO_2 and its effect on photocatalytic degradation of dyes under visible irradiation," *Langmuir*, vol. 24, no. 14, pp. 7338–7345, 2008.